

DTIC FILE COPY

CRREL

REPORT 89-2



4

US Army Corps
of Engineers

Cold Regions Research &
Engineering Laboratory

AD-A206 868

*Airborne radar survey of a brash ice jam
in the St. Clair River*



DTIC
ELECTE
APR 18 1989
S H D

DISTRIBUTION STATEMENT A

Approved for public release;
Distribution Unlimited

89 4 18 052

For conversion of SI metric units to U.S./British customary units of measurement consult ASTM Standard E380, Metric Practice Guide, published by the American Society for Testing and Materials, 1916 Race St., Philadelphia, Pa. 19103.

Cover: Measuring brash ice thickness in the South Channel from the USCG Cutter Bristol Bay.

CRREL Report 89-2

February 1989



Airborne radar survey of a brash ice jam in the St. Clair River

Steven F. Daly and Steven A. Arcone

Prepared for
OFFICE OF THE CHIEF OF ENGINEERS

Approved for public release; distribution is unlimited.

SECURITY CLASSIFICATION OF THIS PAGE

Form Approved
OMB NO. 0704-0188
Exp. Date: Jun 30, 1986

SECURITY CLASSIFICATION OF THIS PAGE

UNCLASSIFIED

PREFACE

This report was prepared by Steven F. Daly, Research Hydraulic Engineer, Ice Engineering Research Branch, Experimental Engineering Division, and Dr. Steven A. Arcone, Geophysicist, Snow and Ice Branch, Research Division, U.S. Army Cold Regions Research and Engineering Laboratory. Funding for this research was provided by DA Project 4A161102AT24, *Research in Snow, Ice, and Frozen Ground*; Task SS, *Combat Service Support*; Work Unit 014, *Electromagnetic and Radiative Characteristics of Snow, Ice, and Frozen Ground*.

This report was technically reviewed by Dr. Kenneth Jezek and Dr. Jean-Claude Tatinclaux of CRREL. The authors express their appreciation to Michael O'Bryan, U.S. Army Engineer District, Detroit, and to Captain Hayden of the U.S. Coast Guard Icebreaker *Bristol Bay* for their assistance in this project; Dr. Robert Wills of Dartmouth College for his assistance in data processing; Allan Delaney of CRREL for his excellent operation of the radar; and Dr. Samuel Colbeck for providing the system for digitizing the photograph of the brash ice.

The contents of this report are not to be used for advertising or promotional purposes. Citation of brand names does not constitute an official endorsement or approval of the use of such commercial products.

Accession For	
NTIS GRA&I	<input checked="" type="checkbox"/>
DTIC TAB	<input type="checkbox"/>
Unannounced	<input type="checkbox"/>
Justification	
By	
Distribution/	
Availability Codes	
Dist	Avail and/or Special
A-1	

CONTENTS

	Page
Abstract	i
Preface	ii
Introduction	1
Objectives and procedures	2
Equipment	2
Radar	2
Brash ice probe	3
Temperature measurements	3
St. Clair River ice conditions	3
Results and discussion	4
Thickness and temperature	4
Size distribution	7
Radar survey	8
Discussion of errors	11
Porosity	11
Phase state of the ice	12
Partial submergence of individual pieces	12
Spectra of reflected energy	12
Conclusions and recommendations	13
Literature cited	13
Appendix A: Laboratory verification of surface scattering from a simulated ice jam	15
Appendix B: Display of digitized and processed data	17

ILLUSTRATIONS

Figure

1. Attenuation rate of radio waves in fresh water as a function of frequency at a conductivity of 0.01 S/m (100- Ω -m resistivity)	1
2. Model 3102 antenna unit mounted off the rescue platform of a Hughes amphibious helicopter	2
3. Typical waveform of a subsurface radar pulse	3
4. Radar echo scan and equivalent graphic display	3
5. Location of study site	4
6. Brash ice cover on the South Channel	5
7. Location of brash ice thickness and water temperature measurements	6
8. Vertical water temperature profiles	7
9. Vertical photograph of brash ice taken from the Bristol Bay	7
10. Absolute frequency histogram of diameters of equivalent area circles for the pieces in Figure 9	8
11. Portions of the analog radar record from open water and brash ice in the South Channel	8
12. Artists concept of how radar reflections form from brash ice	9
13. Comparison of actual open water and brash ice reflected waveforms	10

Figure	Page
14. Calculated brash ice thickness for every ninth of the 1740 scans that compose the brash ice profile of Figure 11	10
15. Histograms of time delays for 184 independent brash ice returns relative to the open water reflections, and brash ice depths as measured with a probe	11
16. Comparison of the Fourier amplitude spectrum of an open water return with the average of 193 spectra of the brash ice returns	12

TABLES

Table

1. Summary of measurements made from USCG Cutter <i>Bristol Bay</i> on 25 February 1987	5
2. Size distribution of brash ice pieces in the South Channel of the St. Clair River on 25 February 1987	8

Airborne Radar Survey of a Brash Ice Jam in the St. Clair River

STEVEN F. DALY AND STEVEN A. ARCONI

INTRODUCTION

The use of short-pulse radar to survey freshwater ice from the air has been reported by several authors (Chizhov et al. 1977, Dean 1977, Batson et al. 1984a,b, Arcone and Delaney 1987, O'Neill 1988). These investigations have clearly shown that short-pulse radar can profile sheet ice thickness and some underlying frazil formations so long as the surface is reasonably smooth. Radar data gathered over brash or rough frazil ice formations in temperate rivers have been reported by Dean (1977) and Batson et al. (1984a,b). Arcone et al. (1986) also conducted a radar study of artificial brash ice made in a lake. Profiling brash ice thickness is important in areas where jams have caused flooding or impeded navigation. However, direct interpretation of subsurface ice formations does not seem possible because of the limited detection sensitivity of commercial radars. The radars used in the above brash ice studies experienced high radiowave attenuation in cold water as well as additional losses from geometric beam spreading and volume and surface scattering. Also, surface ice sheet roughness severely affects subsurface interpretation (e.g., Arcone and Delaney 1987).

In this report we discuss a radar survey using a helicopter-borne UHF antenna to determine brash ice thickness indirectly through interpretation of its freeboard. Small variations in freeboard will correspond to large changes in total ice depth. Such small variations may not be visually apparent, but could be read from a radar record. To determine the accuracy of the radar measurements, we also made simultaneous "ground truth" measurements of brash ice thickness, size distribution and water temperature.

The use of short-pulse radar to probe the depth of brash ice is inhibited by several factors. Brash ice

typically floats in a matrix of highly reflecting and absorbing cold water that permits little radar penetration, as evidenced by the strong attenuation rates seen in Figure 1. Figure 1 shows that even at pulse center frequencies as low as 100 MHz, penetration into 3 m of water (6 m round trip) will cause 24 dB of loss to the reflected waveforms because of surface reflectance and conductive absorption by even relatively "clean" water of 100- Ω -m resistivity. This loss will increase to 35 dB in water with 50- Ω -m resistivity, which is more typical of the larger, heavily used rivers of North America. It seems clear then that pulses centered near 50 MHz or less will be required if penetration of more than a few meters is desired. However, all commercially available antennas that can be feasibly mounted to a small helicopter operate above 100 MHz. Furthermore, any slope in the ice bottom profile greater than about 6° will cause energy reflected back

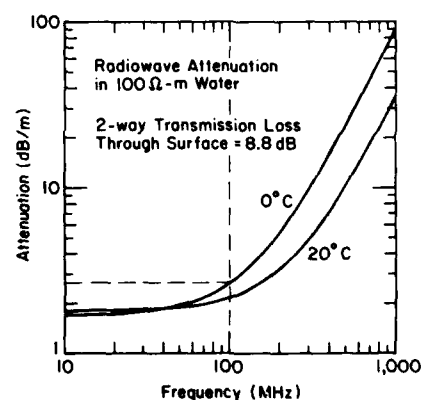


Figure 1. Attenuation rate of radiowaves in fresh water as a function of frequency at a conductivity of 0.01 S/m (100- Ω -m resistivity).

through the water surface to refract into air too severely for detection. Therefore, even from a practical point of view, interpretation of data from below the waterline is not possible.

OBJECTIVES AND PROCEDURES

Our primary objective was to investigate the ability of a short-pulse radar operating in the UHF band (300–3000 MHz) to determine brash ice thickness indirectly by interpreting the mean freeboard height of the brash ice from the radar data. Our hypothesis was that the freeboard height could be extracted from the time delay difference between the leading edges of the incoherent radiation backscattered from the surface of the brash ice and those of the coherent radiation reflected from the water surface. A secondary objective was to see if the spectra of the energy reflected from brash ice would show any correlation with the size distribution or "roughness" of the ice surface. If so, then such information could be used to predict whether or not a different frequency band would give better information.

The brash ice surveyed was a continuous jam in the South Channel of the St. Clair River north of Seaway Island near Lake St. Clair. Data were collected on 25 February 1987 using a 500-MHz center frequency radar pulse waveform radiated from an antenna mounted off the rescue platform of a Hughes-HH-52 amphibious helicopter operated by the Coast Guard. In addition, these data have also been analyzed by Jezek et al. (1988) using a different approach based on scattering theory. Their results will be compared to these in a later section of this report.

EQUIPMENT

Radar

The radar consisted of a Xadar (Springfield, Virginia, now part of Ensco Co.) Electromagnetic Reflection Profiling (control) Unit, a GSSI (Hudson, New Hampshire) model 3102 high frequency antenna, an electrostatic chart recorder (EPC Co., Danvers, Massachusetts) and associated cables and power supplies. The control unit employed a small magnetic tape cassette to record data and the entire radar operated on batteries. Figure 2 shows the 3102 antenna mounted off the rescue platform of the helicopter. The proximity of the metal platform caused several noise bands to appear in the rec-

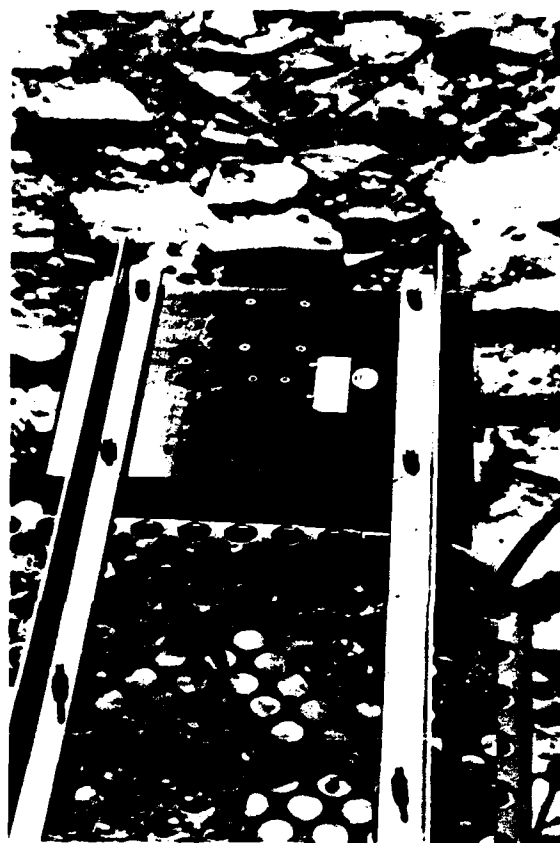


Figure 2. Model 3102 antenna unit mounted off the rescue platform of a Hughes amphibious helicopter.

ords. Recorded data were played back on the EPC chart recorder after the surveys.

The 3102 antenna radiates a short-pulse waveform similar to that in Figure 3. This waveform is maintained over the 70° 3-dB beamwidths in both principal radiation planes (Arcone et al. 1986) when radiated in air. Surface sampling area (or antenna "footprint") depends mainly on these beamwidths, altitude and, to a minor degree, aircraft velocity and scan rate (the inverse of the time taken to compile a scan of echoes). Using the above beamwidths, a mean altitude of 7 m, mean speed of 7 m/s, a scan rate of 8 Hz and the formulation given in Arcone and Delaney (1987), we determined that the average sampling area of our survey was an ellipse of axial lengths 10 by 11 m and roughly 90 m² in area.

An idealized representation of the radar graphic display is shown in Figure 4. Darkness is proportional to signal intensity and a series of bands represent a series of temporally coherent signal returns. These displays are a composite of many

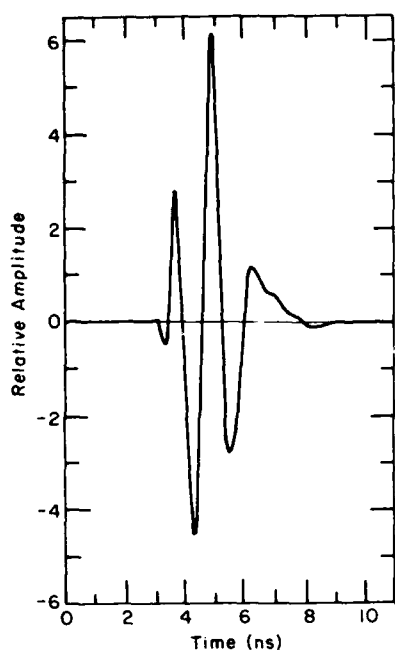


Figure 3. Typical waveform of a sub-surface radar pulse. Time scale is arbitrary.

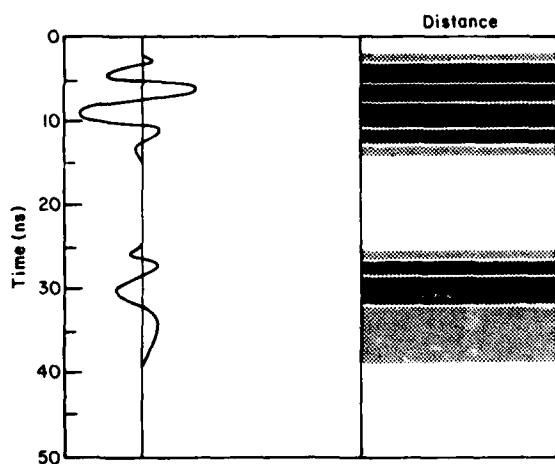


Figure 4. Radar echo scan and equivalent graphic display should these scans remain constant while antenna is moved.

scans, each lasting over an echo time window of 50–200 ns. The scan rate of our control unit was fixed at the rate of eight per second. Generally, the quality of data increases as the helicopter speed and altitude decrease. A flying speed of 2–6 m/s at a height of about 3 m is ideal, but rarely achieved because of wind or surface visibility (e.g., blowing snow) constraints.

Brash ice probe

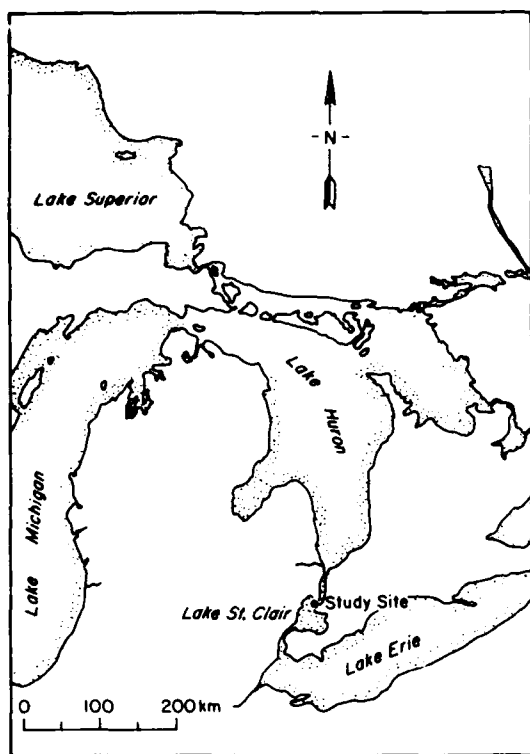
A brash ice probe developed by R. Perham of CRREL was used to measure brash ice thickness from the deck of the USCG Cutter *Bristol Bay*. The probe consists of an aluminum rod with a hinged plate at one end. The probe is driven through the brash ice and the hinged plate is unfolded from the probe. The probe is then lifted until the unfolded plate contacts the underside of the brash ice. The vertical distance between the contacted bottom and the visually estimated top surface of the brash ice is then read from a scale marked on the probe and is the measured total brash ice thickness. The hinged plate is then refolded into position and the probe removed from the ice. Measurements made in this manner are probably accurate to within 5 cm. No measure could be made of the surface height as it was too dangerous to walk on the ice.

Temperature measurements

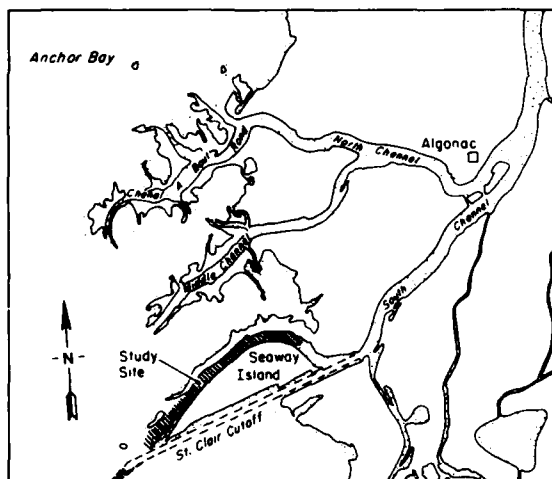
We measured the water temperature using an individually calibrated thermistor, custom mounted in a plastic protector and attached to 15 m of teflon coated cable. The resistance of the thermistor was measured with a handheld Fluke Digital Multimeter, Model 8060A. The resistance was converted to a temperature using the Steinhart-Hart equation with three terms. The nominal accuracy of this system is $\pm 0.02^{\circ}\text{C}$, but in practice, the accuracy approaches $\pm 0.01^{\circ}\text{C}$. The temperatures are recorded to the nearest hundredth of a degree Celsius.

ST. CLAIR RIVER ICE CONDITIONS

The formation of a naturally occurring ice bridge in southern Lake Huron at the entrance of the St. Clair River (Fig. 5a) generally restricts the movement of ice out of Lake Huron. However, northerly winds can disrupt this ice bridge and allow large amounts of ice to enter the St. Clair River. The currents of the St. Clair River carry the ice downstream until they meet the solid ice cover of Lake St. Clair. The movement of the ice is then stopped. Even if there is no solid ice cover in Lake St. Clair, the lack of water current in the lake may stop the movement of ice from Lake Huron. The arriving ice then forms a rough ice cover. The upstream edge of the cover progresses upstream at a rate determined by the rate of arrival of the ice floes and the resulting ice thickness. During normal winters the ice cover in the St. Clair River may progress from the mouth of the river upstream 8 to 16 km. During



a. General area.



b. South Channel radar survey site. Shaded area is the brash ice jam.

Figure 5. Location of study site.

extreme years the river may be ice-covered nearly to Lake Huron.

The rough ice cover formed in the St. Clair River can impede and disrupt vessel traffic and also cause water levels to rise and flood large inhabited areas along the shores of the river. During the

1986–87 winter, when the surveys described in this report were conducted, there were several severe ice jams with related flooding on 24–26 January, 8–11 February, 14–17 February and 10–20 March 1987 (USAED, Detroit 1988). The total damage was estimated at \$1.48 million.

The brash ice that is described in this report originated in Lake Huron. This ice, broken into floes by the wind, arrived at the stationary ice cover where it was then attacked repeatedly by Coast Guard icebreakers, beginning on 28 January. Prior to the survey on 25 February 1988, up to four ice-breaking vessels had been operating in the St. Clair River to relieve flooding.

RESULTS AND DISCUSSION

The radar surveys were carried out on 25 February 1987 along the path shown in Figure 5b, which is the part of the South Channel that runs north of Seaway Island. Altitude was generally 7 m and flight speed was about 7 m/s. Direct measurements were made and photographs (e.g., Fig. 6) of the brash ice were taken on the same day from the *Bristol Bay*. Air temperatures during the surveys ranged between 4.5 and 10°C.

Thickness and temperature

The brash ice thickness and water temperature measurements are summarized in Table 1. The location of the measurements is shown in Figure 7. At each location, the brash ice thickness was measured at several points from the deck of the *Bristol Bay*, from approximately midships to the stern, with an equal number of measurements made on the port and starboard sides. The average thickness at each location ranged from 0.52 to 1.01 m. The range of thickness at any measuring point could be as much as 1.22 m. The maximum thickness was 1.70 m and the minimum was 0.10 m. In the South Channel, thicknesses increased downstream.

The water temperature ranged from 0.95°C in the St. Clair River at Algonac to 0.07°C in the St. Clair Flats Canal. Vertical profiles of water temperature (Fig. 8) reveal a range of water temperature that is less than 0.2°C in the vertical direction, except for the profile in Lake St. Clair where the range is 0.5°C. These are "well mixed" profiles, expected in rivers where the flow velocity generates turbulence that can quickly mix the water in the vertical direction. The somewhat more stratified temperature profile for Lake St. Clair (no. 6) is appropriate in this low velocity region.



Figure 6. Brash ice cover on the South Channel. The cover is dominated by nearly horizontal slabs but vertical and suspended pieces are visible.

Table 1. Summary of measurements made from USCG Cutter *Bristol Bay* on 25 February 1987.

Measure- ment no.	Location	Average water temperature (°C)	Average brash thickness (m)	Maximum brash thicknes (m)	Minimum brash thickness (m)	No. of thickness measurements
1	S. Channel	0.33	0.52	0.70	0.10	11
2	S. Channel	—	0.87	1.30	0.22	8
3	S. Channel	—	0.88	1.20		
4	S. Channel	0.14	1.01	1.70	0.25	7
5	St. Clair Flats Canal	0.07	0.93	1.60	0.30	5
6	Lake St. Clair	0.37	0.92	1.20	0.65	4

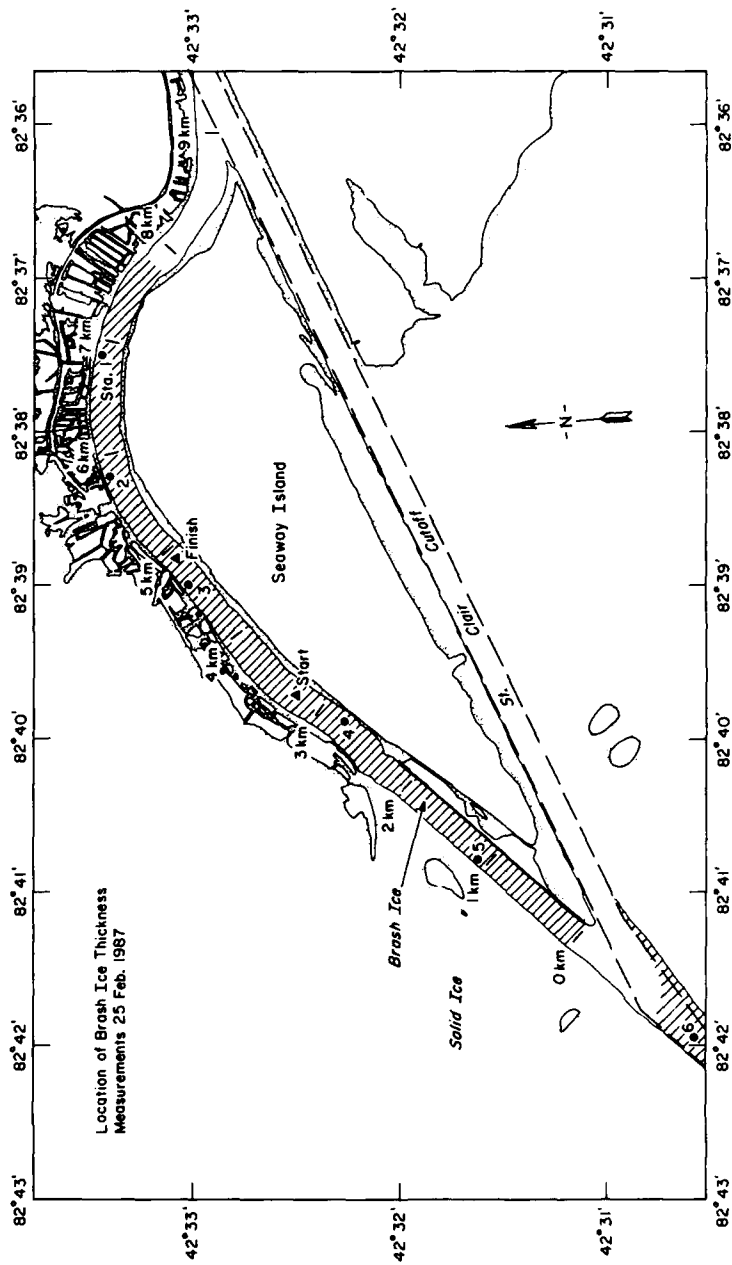


Figure 7. Location of brash ice thickness and water temperature measurements.

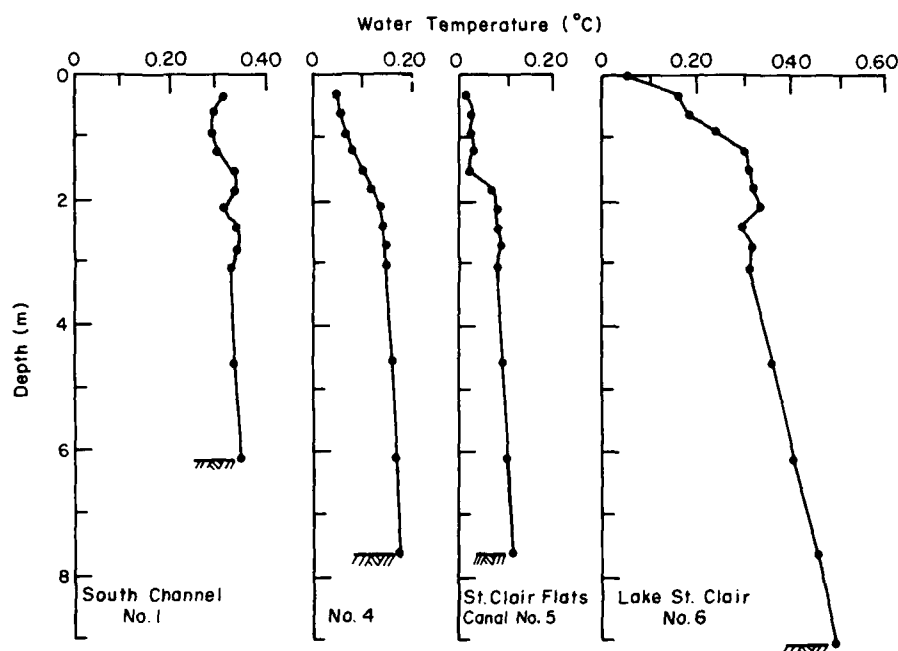


Figure 8. Vertical water temperature profiles.



Figure 9. Vertical photograph of brash ice taken from the Bristol Bay. Scale gradations on rod are 10 cm.

Size distribution

The size distribution of the brash ice was estimated from a photograph (Fig. 9) taken from the deck of the *Bristol Bay*. The photograph looks directly downward at the ice. The brash ice probe was laid horizontally across the ice, the scale marked on the probe providing the scale for the photo. We

made our measurements from the photograph, using a digitizing tablet. As can be seen from Figure 9, the shapes of the brash ice pieces are quite irregular. Submerged portions of a brash ice piece are, of course, not visible, but such portions are not relevant here because they will also be invisible to the radar. Therefore, measurements were made only of the visible portions of each distinct ice piece in the photograph. The size distribution (Table 2) is presented as the mean, standard deviation and range for the diameter of a circle with the equivalent area of each piece and the maximum straight line length that could be found in each piece. A histogram of these results is

shown in Figure 10 along with the best fit log-normal distribution.

The thickness distribution of the pieces was not measured as we had no means to retrieve pieces from the jam. Our visual estimate is that thickness ranged between 5 and 10 cm.

Table 2. Size distribution of brash ice pieces in the South Channel of the St. Clair River on 25 February 1987.

Parameter	Mean (cm)	Standard deviation	Minimum (cm)	Maximum (cm)
Diameter of equivalent circle	15.5	15.5	2.2	92.4
Maximum diameter	18.5	19.5	2.4	109.3

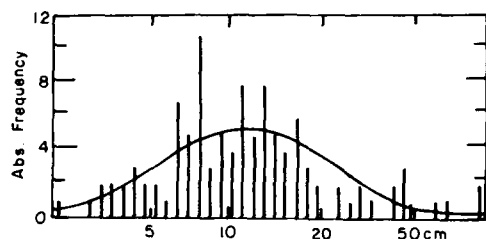


Figure 10. Absolute frequency histogram of diameters of equivalent area circles for the pieces in Figure 9.

Radar survey

Figure 11 shows the portion of the brash ice analog record (along section Start-Finish in Fig. 7) that was analyzed along with a record taken over open water. The dark wavy bands in the open water section are the water surface reflections. The wavy character is caused by the fluctuating altitude of the helicopter. The continuity of the banded structure of the water reflection shows that these reflections were coherent; i.e., the waveform structure of the incident pulse was retained upon reflection. Hori-

zontal bands running across both records result from coherent noise—mainly helicopter reflections.

The reflections from the open water in Figure 11 are highly coherent. The brash ice reflections also show a coherent component, presumably from the water surface, with a weaker superimposed incoherent backscatter. The backscatter, presumably from the brash ice freeboard, arrives first and appears as a "ghost" reflection above the water reflection. There is no

evidence of any later reflections from the bottom of the brash ice and no later reflections were seen on larger time scales. We expected this at the pulse center frequency of 500 MHz because of the high conductive and dielectrically absorptive attenuation rate (~ 22 dB/m) in water near 0°C and because of the additional losses caused by scattering on the surface and within the volume of the brash ice thickness.

We believe that surface scattering is the major cause of the incoherent event seen in Figure 11. This assumption is so crucial to our freeboard measurement hypothesis that a laboratory experiment has been conducted on a simulated ice jam to reproduce and verify this effect. The results have been positive and are discussed in Appendix A.

It therefore seems possible that if the time delay, t_d , between the onset of the incoherent and coherent components could be measured, we could then translate t_d into freeboard height and, from this, estimate the total brash ice depth. Figure 12 gives the conceptual basis for this approach. The brash ice reflection is presumed to be the superposition of surface scatter and a time delayed coherent reflection, mainly from the melted and near horizontal

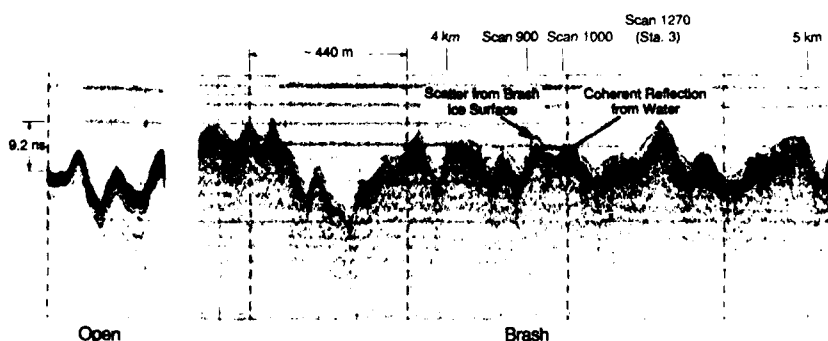


Figure 11. Portions of the analog radar record from open water (coherent) and brash ice (partially coherent) in the South Channel. The brash ice record contains 1740 scans.

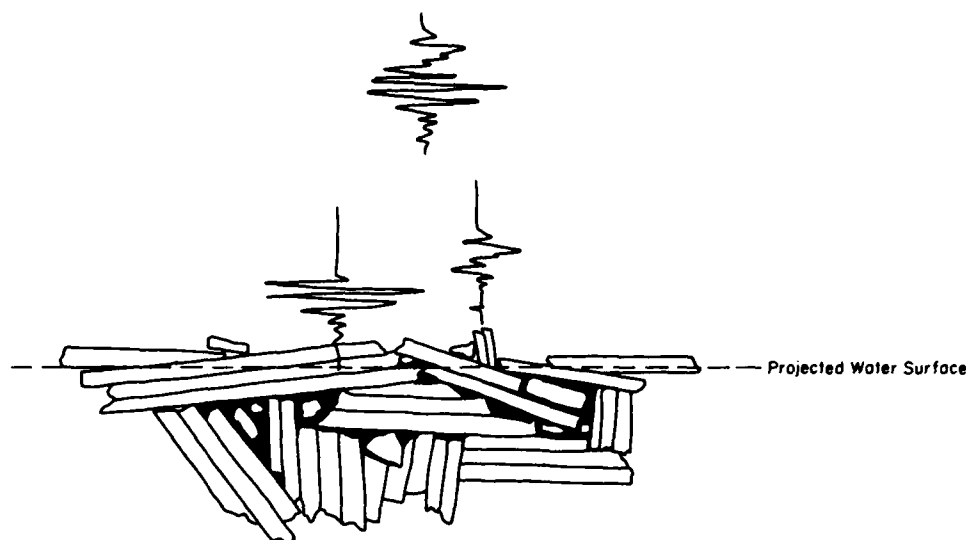


Figure 12. Artists concept of how radar reflections form from brash ice; a superposition (top waveform) of reflections from the interfacial water with those from the surface of the brash ice pieces.

water surfaces sandwiched between the rafted ice pieces. The surface scatter is presumed weaker because of the rough ice surface. It will have an unknown waveform, but it will have a recognizable leading edge. Thus, the dominant oscillations of the brash ice waveforms can be matched to those of the open water waveforms to determine the time delay, t_d , of the earliest arriving brash ice backscatter, as will be seen next. Two necessary assumptions regarding the reflections from the water surface are 1) that they represent energy that has propagated primarily through ice, and 2) that the stronger oscillations are weakly affected by the surface scatter of the brash ice. We do not know the degree to which the coherent component of the reflections originated from the open water visible between the ice pieces. However, given the relatively small area of exposed water (Fig. 9), and that an open water reference for measuring t_d gives more than twice the measured ice thickness because of the air path for the coherent energy, the first assumption seems sound.

The durations of the transmitted waveforms are too long to permit us to clearly separate scatter from the top of the brash ice from the reflections from the water surfaces. Also, helicopter clutter is superimposed on the entire record. Therefore, the analog record of Figure 11 was digitized and the average amplitude distribution of all scans was removed from each scan to reduce noise so that the individual scans could be examined to determine the local freeboard height. Figure 13 presents a few of these scans. The waveforms are superimposed

on a reference open water waveform by aligning the strongest oscillations. Appendix B presents a display of a small portion of Figure 11 that uses 100 consecutive scans.

The return of Figure 13a differs little from that of the open water and, therefore, indicates that the surface sampling area of about 90 m² had little or no brash ice. Figures 13b through d, however, show returns from the brash ice, ranging from 0.7 to 1.0 ns earlier than the superimposed open water reflection. The extended oscillation in the brash ice waveforms represents an interference between the water surface and brash ice returns. Using the simple formula for depth

$$d = \frac{ct_d}{2n} \quad (1)$$

where t_d = time delay
 n = refractive index (1.79 for ice)
 c = 30 cm/ns

and with an estimated reading accuracy of ± 0.1 ns, we translate these time delays into brash ice freeboard heights of 5.9 (± 0.8) to 8.4 (± 0.8) cm. Then, assuming that the brash ice weight and buoyancy forces are in equilibrium over the sample area, that the porosity of the brash ice is the same above the water as below, and that the density of the individual brash ice pieces was 0.916 (the individual pieces are solid), these freeboard heights give a total brash ice thickness of 70 (± 10) to 100 (± 10) cm.

The actual variation of computed total brash ice

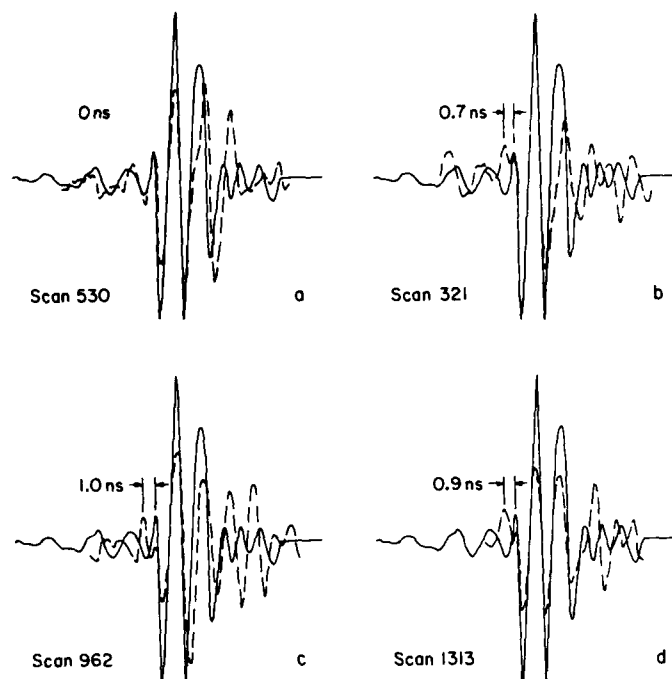


Figure 13. Comparison of actual open water (solid) and brash ice (dashed) reflected waveforms. Waveforms have been aligned by the large coherent oscillations, thus revealing the earlier arrival of the brash ice returns.

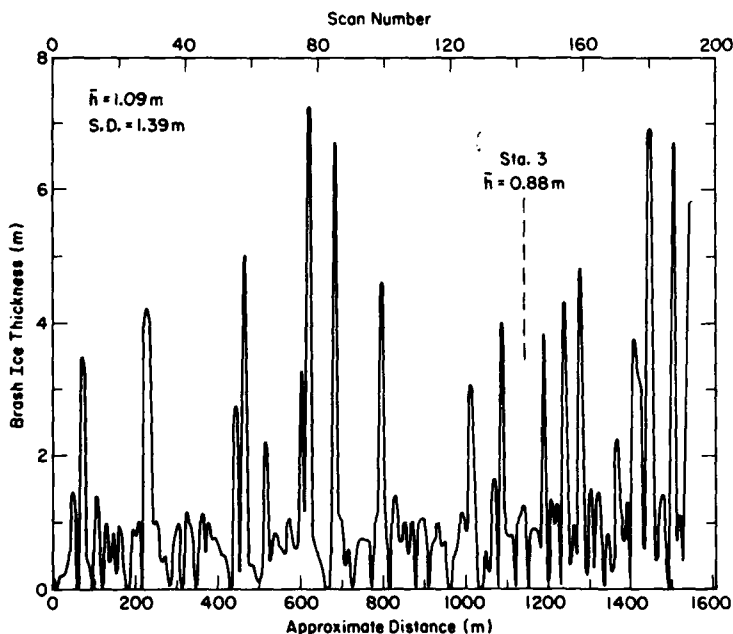
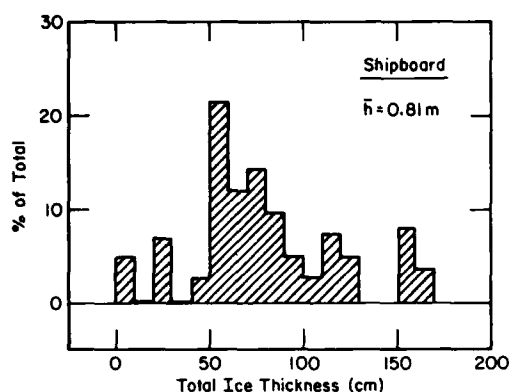
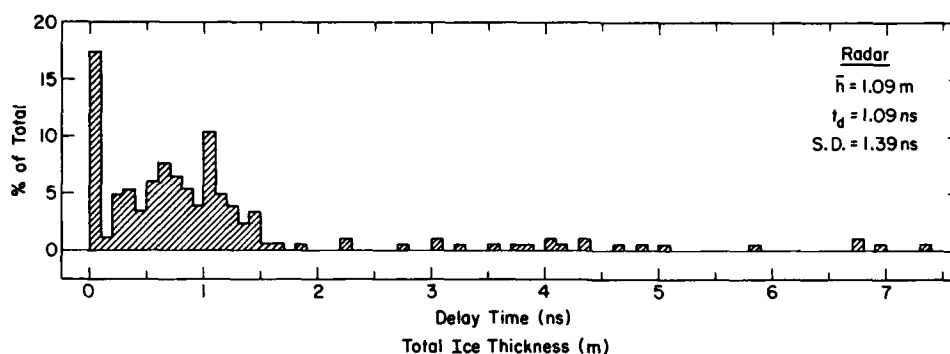


Figure 14. Calculated brash ice thickness for every ninth of the 1740 scans that compose the brash ice profile of Figure 11. The actual scan number is found by multiplying the given number by 9.

thickness, given the assumptions stated above, along the profile of Figure 11 is presented in Figure 14. The values were computed from 193 scans, 9 of which could not be interpreted and so are interpolated. Each scan is spaced nine scans apart to give some statistical independence to each area of brash ice being sampled; the centers of the areas are thus separated by about 8 m. There are many large deviations from the average of 1.09 m (± 0.1) and several calculations of 0.00-m thickness. Figure 15 gives a histogram of these values and compares them with a histogram of all shipboard measurements. There is a strong peak at 0.0- to 0.1-ns delay, which represents reflections from open water or water over submerged ice. A second peak occurs at 1.0 to 1.1 ns and this is where the average (1.09 ns) of all samples occurs also. Only 12.5% of all values fall above 2.0 ns. The average value of 1.09 ns translates to 9.1-cm freeboard height. The average estimated



a. Shipboard measurements.



b. Radar measurement.

Figure 15. Histograms of time delays for 184 independent brash ice returns relative to the open water reflections, and brash ice depths as measured with a probe. The numerical equivalency of \bar{h} and t_d is coincidental.

total thickness of brash ice of about $109 (\pm 10)$ cm is more than the average measured thickness of 92 cm of stations 2, 3 and 4, which were located on or close to the reach over which the helicopter survey was conducted. The freeboard height of 9.1 cm is in fair agreement with the rms roughness of 12 cm estimated by Jezek et al. (1988) for this same data set.

DISCUSSION OF ERRORS

The disagreement between the calculated and measured brash ice thicknesses can be related to observation errors and to incorrect assumptions used in the radar data processing. The observation errors are the inaccuracies of the visual determinations of 1) the height placement of the top surface of the ice on the ice probe, and 2) the time delay, t_d , between the brash ice backscatter and the coherent water reflection. As stated above, the direct probe measurements are estimated to be accurate to within 5 cm and the time delays to within 0.1 ns, which translates to about 10 cm of total ice depth. This margin of error can bring the average probe depths for stations 2, 3 and 4 up to 97 cm and the radar

determined average depth for the survey section of Figure 11 down to 99 cm.

The assumptions used in the radar processing that may be incorrect are 1) that there is equal ice porosity above and below the water line, 2) that the individual ice pieces are solid ice, and 3) that water reflections occur at the mean water level. The first two factors relate to the correct effective refractive index that should be used in eq 1. The calculations assumed solid ice with no porosity, which is obviously wrong. The third factor relates to exactly where the coherent water reflections originated, as was depicted in Figure 12.

Porosity

Neglecting the weight of air, we can simply calculate the ratio of the freeboard height, h_f , to the total thickness, h , by assuming a vertical equilibrium of force as

$$\frac{h_f}{h} = \frac{\left(1 - \frac{\rho_i}{\rho_w}\right)}{\left(\frac{\rho_i}{\rho_w} \left(\frac{1 - e_f}{1 - e_b}\right) - 1\right) + 1} \quad (2)$$

where r_i = density of ice
 r_w = density of water
 e_f = porosity of the freeboard ice
 e_b = porosity of ice below the water line.

For the calculated and measured brash ice thicknesses to coincide, and assuming the radar could measure the brash ice freeboard accurately, the freeboard porosity and the porosity below the water line would have to differ. There are no direct measurements in the St. Clair River or at other locations—the Gulf of Bothnia, for example (Sandquist 1986)—that support such a difference in porosities. However, the continual sifting of small brash ice pieces down through the freeboard as the brash ice moved and was attacked by icebreakers could tend to decrease the porosity of the ice below the water line and increase the porosity in the freeboard. As the porosity of the brash ice is probably in the range of 0.3 to 0.6 (Fig. 6), such a difference in porosity is not hard to imagine. Further field measurements are required to resolve this issue.

In any case, the freeboard porosity was not used in the calculation of the freeboard thickness as determined by eq 1. If the porosity is greater than zero above the water line, then the use of the solid ice value, n (1.79), in eq 1 used to translate t_g into an ice thickness will give a smaller value of the freeboard thickness than would an n adjusted to account for porous ice ($1 \leq n \leq 1.79$). As an example, a more accurate but simple volumetrically based mixing formula for n adjusted for a porosity of 0.5 would increase the calculation of total ice thickness by about 19%.

Phase state of the ice

The second factor contributing to the difference in measured and calculated values is the state of the individual ice pieces. The use of $n = 1.79$ in eq 1 presumed the ice to be solid. However, the unseasonably warm weather probably caused wetting along crystal grain boundaries, which would lead to an increase in n to as high as 2.0 (Arcone et al. 1986). Under such conditions the calculated brash ice thickness increases by about 11% when data are processed under the assumption of no porosity and $n = 1.79$.

Partial submergence of individual pieces

Most pieces at the surface must be partially submerged so that the coherent reflections originate from the bottoms of the brash ice pieces, which are below the projected waterline (as illustrated in Fig. 12). This would increase the delay between coherent and incoherent reflections and lead to a positive error in the calculated brash ice thickness. A negative correction of 1.4 cm from the calculated average freeboard height of 9.1 cm is required to give the 92-cm value of total brash ice thickness measured from the ship at stations 2–4. This correction amounts to 28% of the thickness of a 5-cm-thick piece and 14% of a 10-cm piece. In general, however, for a free floating column of stacked slabs, the percent overestimate of total thickness is proportional to the bottom depth of the highest submerged slab, a quantity that will vary as more slabs are added. As an example, a stack of ten 10-cm-thick slabs will give a radar overestimate of 33% in the total thickness because of the partial submergence of the top slab.

SPECTRA OF REFLECTED ENERGY

Figure 13 revealed a slight frequency shift in some of the reflected brash ice waveforms relative to the open water reference waveform because the

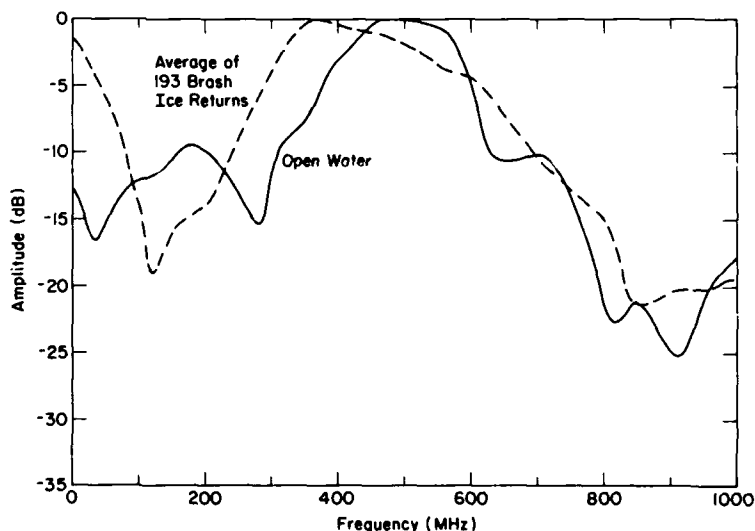


Figure 16. Comparison of the Fourier amplitude spectrum of an open water return with the average of 193 spectra of the brash ice returns.

oscillation periods lengthened (e.g., Fig. 13b and 13c) from left to right. This shift can be seen also in Figure 16, in which the average amplitude spectrum of every ninth of the 1740 scans of the brash ice portion of Figure 11 is compared with the amplitude spectrum of the open water reflection. Here we see that the strongest brash ice component occurs at about 370 MHz, as compared with about 480 MHz for the open water reflection waveform. This frequency shift seems to be attributable to a greater loss of energy in the 400- to 600-MHz frequency range in the reflected radar pulse waveform; i.e., the brash ice pieces seem to selectively scatter the frequency components around 500 MHz and thus diffuse this energy away from the receiver. The frequency for conducting spheres to give maximum backscatter that corresponds to the mean diameter of 15.5 cm is about 600 MHz ($c + \text{circumference}$) so that our radar does operate in the right frequency range for selective backscatter. However, the theory is not so well established for dielectric disks whose diameters are on the order of a wavelength (Ruck 1970) that we can predict what frequencies will be dispersed. Figure 16 also shows that there is little degradation of the frequency content above 600 MHz so that one would not expect this scattering process to have degraded the leading edge of the backscatter significantly.

CONCLUSIONS AND RECOMMENDATIONS

The present UHF short-pulse radar appears capable of mapping relative changes in brash ice depth. Empirical adjustments based on measurements of the brash ice porosities above and below the water line and of individual brash ice piece thickness and refractive index would be required to give more accurate calculations of brash ice thickness. A quantitative picture may not be important, however, if only regions of extreme thickness are sought.

Data interpretation using only the analog record seems feasible as long as the onset of surface backscatter and the major oscillations (bands on the analog record) can be identified. The major obstacle to this is noise reduction, for which the following two steps are recommended.

1. Use of short fiber optic cables between the control unit and transmitter-receiver in the antenna housing.

2. Elimination of coherent noise through the use of background removal programs.

Background removal seeks to reduce coherent noise (clutter) by finding the average amplitude distribution across a series of scans and then subtracting it from all scans. Hardware to perform this function is available. For future surveys we plan to record data at a high altitude to isolate helicopter clutter, and then subtract this clutter from the low altitude survey.

The spectral analysis showed that the loss of high frequency components in the total returned signal was compatible with the size distribution of the individual pieces. It is inconclusive, however, as to whether a different frequency radar would give better results. A lower frequency will give a stronger water reflection, but weaker surface scatter and therefore a decreased ability to separate the brash ice return from that of the water surface. A higher frequency will give a weaker water reflection with perhaps too much loss of high frequency content to allow an open water reflection to be matched to the coherent part of the brash ice return. Therefore, the UHF band used may have been an optimum choice for studying brash ice freeboard.

LITERATURE CITED

- Arcone, S. A. and A. J. Delaney (1987) Airborne river-ice thickness profiling with helicopter-borne short-pulse radar. *Journal of Glaciology*, 33(15):330-340.
- Arcone, S. A., A. J. Delaney and R. Perham (1986) Short pulse radar investigations of freshwater ice sheets and brash ice. USA Cold Regions Research and Engineering Laboratory, CRREL Report 86-6.
- Batson, G., H. T. Shen and R. Ruggles (1984a) Investigation of ice conditions in the St. Lawrence River 1983-84. Clarkson University Report No. DTSL55-C-C0085, prepared for St. Lawrence Seaway Development Corporation.
- Batson, G., H. T. Shen and S. Hung (1984b) Multi-year experience of remote sensing of ice thickness on the St. Lawrence River. *Proceedings of the Eastern Snow Conference*, 41st annual meeting.
- Chizhov, A. N., V. G. Glushnev and B. D. Slutsker (1977) A pulsed radar method of measuring ice-cover thickness. *Meteorologiya i Gidrologiya*, 4:90-96 (in Russian).
- Dean, A.M. Jr. (1977) Remote sensing of accumulated frazil and brash ice in the St. Lawrence River.

USA Cold Regions Research and Engineering Laboratory, CRREL Report 77-8.

Jezek, K. C., S. A. Arcone, S. Daly and R. Wills (1988) Impulse radar studies of interface roughness. *Proceedings: Workshop on Ground Probing Radar, May 24-26, Ottawa, Canada.*

O'Neill, K. (1988) Detection of thin layers using short pulse radar. *Proceedings: International Conference on Numerical Methods for Water Resources, Cambridge, Massachusetts: Massachusetts Institute of Technology.*

Ruck, G. T. (ed.) (1970) *Radar Cross Section Handbook*, Vol. 1. New York: Plenum Press, p. 291.

Sandkvist, J. (1986) Brash ice behavior in frequented ship channels. Licentiate Thesis. Series A, no. 139, Water Resources Engineering, Luleå University, Sweden.

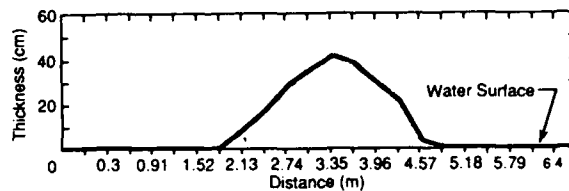
U.S. Army Engineer District, Detroit (1988) After action report on the implementation of the Great Lakes connecting channels ice management plan for the winter of 1986-1987. U.S. Army Corps of Engineers, Detroit, Michigan.

APPENDIX A: LABORATORY VERIFICATION OF SURFACE SCATTERING FROM A SIMULATED ICE JAM

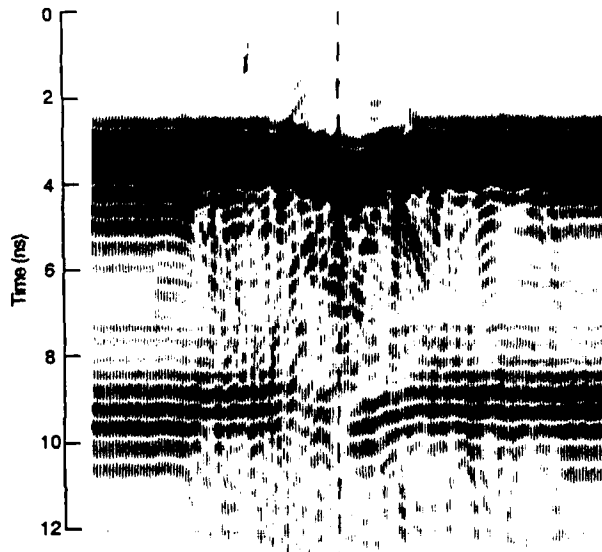
A laboratory simulation of a brash ice jam was profiled by radar to reproduce and thus verify the incoherent surface scatter and the water reflection identified in Figure 11. A 3.7-m wide channel was filled with water to a depth of 1.5 cm. About 2 m³ of polyethylene ($n = 1.48$) pieces, 0.64 cm thick, were then mounded to a height of 35–42 cm across the channel and profiled with a GSSI model 101C radar antenna unit. This unit radiates a waveform almost identical to that of Figure 3, but at about two-thirds the time duration. The frequency of maximum power is about 900 MHz.

Figure A1a gives a cross section of the mound. The structure was visibly porous, with many pieces ranging in orientation from vertical (on edge) to horizontal. In particular, the surface pieces at the top of the mound were close to vertical. Figure A1b gives the corresponding radar profile. The continuous dark bands are the water reflections, which dip beneath the "jam" because of the extended propagation time in the polyethylene. Using the vertical time scale, we see that this dip is only an extra 0.5- to 0.7-ns delay beyond the reflections from the open water (these below-mound reflections are probably formed by refraction around the peak of the mound). An added delay of 0.5 ns represents a dielectric constant (n^2) of 1.47, or conversely, a mound height of only 15.6 cm if we assume the dielectric constant of the mound to be 2.3 as it is for solid polyethylene. Of course, the mound was not solid but was in fact highly porous. Using a dielectric mixing formula based on simple volumetric proportions, we see that the effective dielectric constant of 1.47 suggests that porosity was approximately 60%.

The returns from the mound are weaker than those from the water and show less coherence (weaker band structure), especially over the top of the mound where the rough surface produced a sufficiently diffuse scatter to make the earliest re-



a. Cross section.



b. Radar profile.

Figure A1. Polyethylene simulation of a brash ice jam.

turns from the peak undetectable. Nevertheless, the results show that our interpretation of Figure 11 is qualitatively correct: the incoherent event is the surface scatter, the coherent event is the underlying water level, and the time delay between these two events is related to freeboard height. Not accounting for porosity leads to an under-estimate of freeboard height as discussed in the text.

APPENDIX B: DISPLAY OF DIGITIZED AND PROCESSED DATA

This appendix discusses an improved data display that enhances recognition of sudden, large changes in freeboard compared to the conventional graphic display of Figure 11. The 1740 scans of Figure 11 were first digitized over the last 70 ns of each scan, as only this portion contained the brash ice information. Of these scans, 100 (numbers 901-1000 indicated in Fig. 11) were selected for further processing. The average amplitude distribution for all of these scans was subtracted from each scan, and then only the positive polarity amplitude was displayed (Fig. A1). In Figure B1, the technique of hidden line removal has been applied so that any part of a plotted scan that occurs behind another plot (plotting is from bottom to top) is not seen. This procedure produces a less complicated graph allowing the important brash ice features to be easily identified.

In Figure B1, starting from the left side, we see two events common to almost every scan. The first event is of smaller amplitude and is the stronger half cycle oscillation of the brash ice backscatter. This event is followed by a flat valley and then an even stronger half cycle of the coherent water reflection. The remaining half cycles are of no interest as they represent the volume scattering within the brash ice and surface scattering off the beam axis. The separation between the first two half cycles is qualitatively related to brash ice freeboard height. Close examination will show

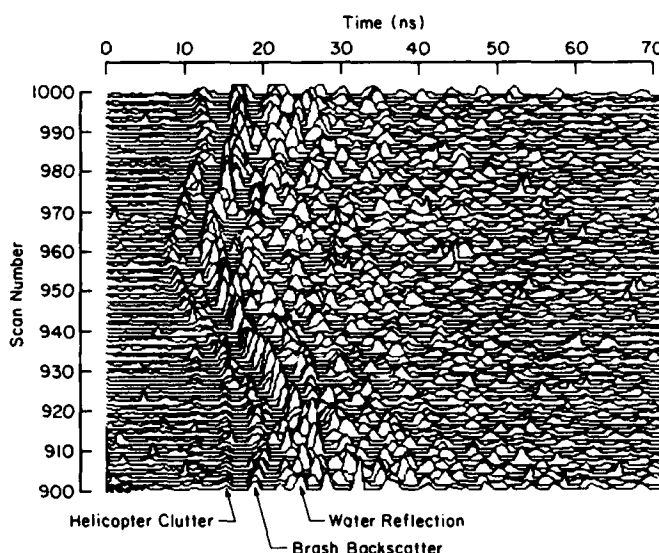


Figure B1. Display of amplitude versus time plots with hidden lines removed for scans 901-1000 approximately located on Figure 11. Background removal has been applied and only positive polarity is printed.

a few scans (e.g., 956 and 996) to contain larger separations between the onsets of both events and some (e.g., 912 and 983) much less. The general waviness is caused by helicopter altitude changes. A logical next step would be to automate the calculation of peak separation. However, it is not clear how to distinguish the desired signal peaks from the undesired noise peaks that still remain.

A facsimile catalog card in Library of Congress MARC format is reproduced below.

Daly, Steven F.

Airborne radar survey of a brash ice jam in the St. Clair River / by Steven F. Daly and Steven A. Arcone. Hanover, N.H.: U.S. Army Cold Regions Research and Engineering Laboratory; Springfield, Va.: available from National Technical Information Service, 1989.

iv, 25 p., illus., 28 cm. (CRREL Report 89-2.)

Bibliography: p. 13.

1. Brash ices. 2. Ice jams. 3. Radar. 4. Radar profiling. 5. River ice. 6. St. Clair River. I. Arcone, Steven A. United States Army. III. Corps of Engineers. IV. Cold Regions Research and Engineering Laboratory. V. Series: CRREL Report 89-2.